NMDA receptor-dependent $GABA_B$ receptor internalization via CaMKII phosphorylation of serine 867 in $GABA_{B1}$

Nicole Guetg[a,1], Said Abdel Aziz[a,1], Niklaus Holbro[b], Rostislav Turecek[a,c], Tobias Rose[b], Riad Seddik[a], Martin Gassmann[a], Suzette Moes[d], Paul Jenoe[d], Thomas G. Oertner[b], Emilio Casanova[a,2], and Bernhard Bettler[a,3]

[a]Department of Biomedicine, Institute of Physiology, Pharmazentrum, University of Basel, 4056 Basel, Switzerland; [b]Friedrich Miescher Institute for Biomedical Research, 4058 Basel, Switzerland; [c]Institute of Experimental Medicine, Academy of Sciences of the Czech Republic, 142 20 Prague, Czech Republic; and [d]Biozentrum, University of Basel, 4056 Basel, Switzerland

Edited* by Richard L. Huganir, Johns Hopkins University School of Medicine, Baltimore, MD, and approved June 24, 2010 (received for review January 22, 2010)

$GABA_B$ receptors are the G-protein–coupled receptors for GABA, the main inhibitory neurotransmitter in the brain. $GABA_B$ receptors are abundant on dendritic spines, where they dampen postsynaptic excitability and inhibit Ca^{2+} influx through NMDA receptors when activated by spillover of GABA from neighboring GABAergic terminals. Here, we show that an excitatory signaling cascade enables spines to counteract this $GABA_B$-mediated inhibition. We found that NMDA application to cultured hippocampal neurons promotes dynamin-dependent endocytosis of $GABA_B$ receptors. NMDA-dependent internalization of $GABA_B$ receptors requires activation of Ca^{2+}/Calmodulin-dependent protein kinase II (CaMKII), which associates with $GABA_B$ receptors in vivo and phosphorylates serine 867 (S867) in the intracellular C terminus of the $GABA_{B1}$ subunit. Blockade of either CaMKII or phosphorylation of S867 renders $GABA_B$ receptors refractory to NMDA-mediated internalization. Time-lapse two-photon imaging of organotypic hippocampal slices reveals that activation of NMDA receptors removes $GABA_B$ receptors within minutes from the surface of dendritic spines and shafts. NMDA-dependent S867 phosphorylation and internalization is predominantly detectable with the $GABA_{B1b}$ subunit isoform, which is the isoform that clusters with inhibitory effector K^+ channels in the spines. Consistent with this, NMDA receptor activation in neurons impairs the ability of $GABA_B$ receptors to activate K^+ channels. Thus, our data support that NMDA receptor activity endocytoses postsynaptic $GABA_B$ receptors through CaMKII-mediated phosphorylation of S867. This provides a means to spare NMDA receptors at individual glutamatergic synapses from reciprocal inhibition through $GABA_B$ receptors.

γ-aminobutyric acid | spines | trafficking | synaptic plasticity | GABAB

$GABA_B$ receptors modulate the excitability of neurons throughout the brain. They are therapeutic targets for a variety of disorders, including cognitive impairments, addiction, anxiety, depression, and epilepsy (1). Depending on their subcellular localization $GABA_B$ receptors exert distinct regulatory effects on synaptic transmission (2–4). Presynaptic $GABA_B$ receptors inhibit neurotransmitter release (5, 6). Postsynaptic $GABA_B$ receptors dampen neuronal excitability by gating Kir3-type K^+ channels, which generates slow inhibitory postsynaptic potentials and local shunting (7). Molecular diversity in the $GABA_B$ system arises from the $GABA_{B1a}$ and $GABA_{B1b}$ subunit isoforms, both of which combine with $GABA_{B2}$ subunits to form heteromeric $GABA_{B(1a,2)}$ and $GABA_{B(1b,2)}$ receptors (8). Genetically modified mice revealed that the two receptors convey nonredundant synaptic functions at glutamatergic synapses, owing to their differing distribution to axonal and dendritic compartments (3, 9). Selectively $GABA_{B(1a,2)}$ receptors control the release of glutamate, whereas predominantly $GABA_{B(1b,2)}$ receptors activate postsynaptic Kir3 channels in dendritic spines (10–12). Activation of $GABA_B$ receptors on spines inhibits NMDA receptors through hyperpolarization and the PKA pathway, which enhances Mg^{2+} block (13, 14) and reduces Ca^{2+} permeability (15) of NMDA receptors. Reciprocally, there is evidence that glutamate receptors decrease surface expression of $GABA_B$ receptors (16–18). This supports that glutamate receptors and $GABA_B$ receptors cross-talk in dendrites and spines.

Neither the glutamate receptors nor the signaling pathways controlling surface availability of $GABA_B$ receptors have yet been identified. Here we show that NMDA receptor-dependent phosphorylation via CaMKII targets $GABA_B$ receptors for internalization. This postsynaptic regulation of $GABA_B$ receptors has implications for the control of local excitability and Ca^{2+}-dependent neuronal functions.

Results

NMDA Receptors Mediate $GABA_B$ Receptor Internalization. We used transfected cultured hippocampal neurons to identify the glutamate receptors regulating cell surface expression of $GABA_B$ receptors. Robust cell surface expression of tagged $GABA_{B1b}$ subunits (HA-GB1b-eGFP) was observed upon cotransfection with $GABA_{B2}$ subunits (Fig. 1*A*), which are mandatory for $GABA_{B1}$ surface expression (8, 19, 20). $GABA_{B1b}$ surface expression was monitored by immunolabeling of the extracellular HA-tag before permeabilization of cells (red fluorescence). Total $GABA_{B1b}$ expression was monitored by immunolabeling of the intracellular eGFP-tag after permeabilization of cells (green fluorescence). To quantify the level of surface $GABA_{B1b}$ protein, we calculated the ratio of red to green fluorescence intensity (Fig. 1 *B* and *C*). Upon glutamate treatment (50 μM glutamate/5 μM glycine for 30 min), surface $GABA_{B1b}$ protein was significantly reduced (41.4 ± 5.3% of control, $n = 10$, $P < 0.001$), consistent with published data (18). The NMDA receptor antagonist APV (100 μM for 2 h) prevented the glutamate-induced decrease in surface $GABA_{B1b}$ protein (98.4 ± 12.6% of control, $n = 9$, $P > 0.05$). We tested whether a selective activation of NMDA receptors is sufficient to decrease surface $GABA_{B1b}$ protein. Following NMDA treatment (75 μM NMDA/5 μM glycine for 3 min) and recovery in conditioned medium for 27 min, surface $GABA_{B1b}$ protein was significantly reduced (54.8 ± 3.2% of control, $n = 10$,

Author contributions: N.G., S.A.A., N.H., R.T., T.R., R.S., M.G., P.J., E.C., and B.B. designed research; N.G., S.A.A., N.H., R.T., T.R., R.S., S.M., and E.C. performed research; T.G.O. contributed new reagents/analytic tools; N.G., S.A.A., N.H., R.T., T.R., R.S., M.G., S.M., P.J., and E.C. analyzed data; and N.G., M.G., and B.B. wrote the paper.

The authors declare no conflict of interest.

*This Direct Submission article had a prearranged editor.

[1]N.G. and S.A.A. contributed equally to this work.

[2]Present address: Ludwig Boltzmann Institute for Cancer Research, A-1090 Vienna, Austria.

[3]To whom correspondence should be addressed. E-mail: bernhard.bettler@unibas.ch.

This article contains supporting information online at www.pnas.org/lookup/suppl/doi:10.1073/pnas.1000909107/-/DCSupplemental.

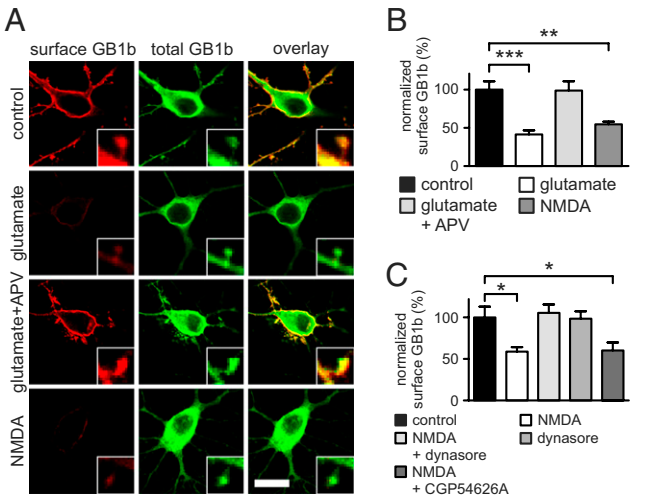

Fig. 1. NMDA-dependent removal of surface $GABA_B$ receptors. (*A*) Rat hippocampal neurons coexpressing exogenous HA-GB1b-eGFP and $GABA_{B2}$ were treated at DIV14 as indicated. Surface $GABA_{B1b}$ (GB1b) protein was fluorescence-labeled with anti-HA antibodies before permeabilization. Total GB1b protein was fluorescence-labeled with anti-eGFP antibodies after permeabilization. Single optical planes captured with a confocal microscope are shown. (Scale bar, 15 μm.) (*Insets*) Representative spines at higher magnification. (*B*) Surface $GABA_{B1b}$ protein was quantified by the ratio of surface to total fluorescence intensity. Values were normalized to control values in the absence of any pharmacological treatment. Surface $GABA_{B1b}$ protein was significantly decreased following glutamate or NMDA treatment. No significant reduction was observed with glutamate treatment after preincubation with APV. $n = 9$–10, $^{**}P < 0.01$, $^{***}P < 0.001$. (*C*) Dynasore but not CGP54626A prevented the NMDA-induced reduction of surface $GABA_{B1b}$ protein. $n = 8$–10, $^{*}P < 0.05$. Quantification was from nonsaturated images. Data are presented as mean ± SEM.

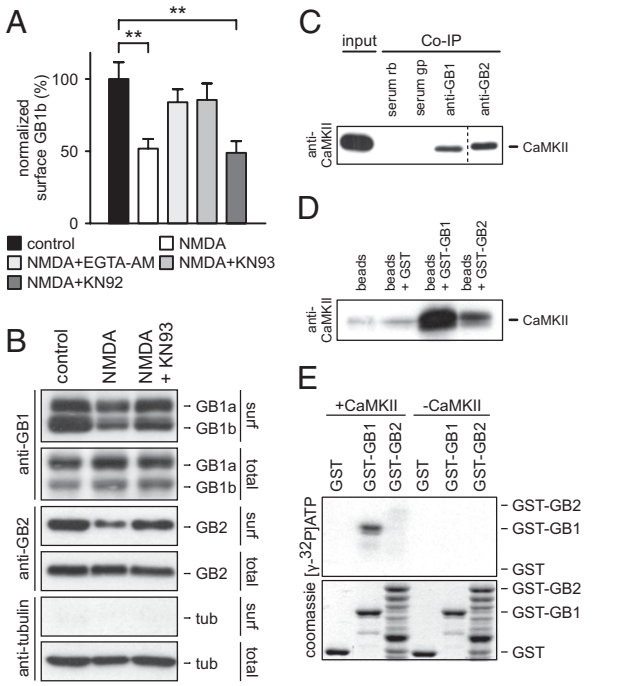

Fig. 2. NMDA-induced removal of surface $GABA_B$ receptors requires CaMKII. (*A*) Rat hippocampal neurons coexpressing exogenous HA-GB1b-eGFP and $GABA_{B2}$ were analyzed at DIV14. Surface $GABA_{B1b}$ protein was quantified by the ratio of surface to total fluorescence intensity. Preincubation of neurons with the Ca^{2+}-chelator EGTA-AM or the CaMKII inhibitor KN-93 prevented the NMDA-induced reduction in surface $GABA_{B1b}$ protein. KN-92 was ineffective. Data are means ± SEM, $n = 9$–10, $^{**}P < 0.01$. (*B*) NMDA-mediated removal of endogenous surface $GABA_B$ receptors. Live cortical neurons were treated at DIV14 as indicated and then biotinylated. Cell homogenates (total) and avidin-purified cell surface proteins (surf) were probed on Western blots with anti-$GABA_{B1}$ (anti-GB1) and anti-$GABA_{B2}$ (anti-GB2) antibodies. While all $GABA_B$ subunits were removed from the cell surface in response to NMDA, $GABA_{B1b}$ was more efficiently removed than $GABA_{B1a}$ ($P < 0.05$). NMDA-mediated removal of surface protein was inhibited by KN-93. Anti-tubulin antibodies were used as a control. Of note, we consistently observed that significantly more $GABA_{B1b}$ protein was detected at the cell surface under control conditions, albeit $GABA_{B1a}$ is more abundant in cortical neurons (GB1a-to-GB1b ratio: surface, 0.71 ± 0.08; total, 1.32 ± 0.05; $n = 3$, $P < 0.01$). (*C*) CaMKII interacts with $GABA_B$ receptors in the brain. Anti-GB1 and anti-GB2 antibodies coimmunoprecipitated CaMKII from purified mouse brain membranes, whereas control rabbit (serum rb) or guinea-pig serum (serum gp) did not. (*D*) Pull-down assays with GST-fusion proteins containing the entire C-terminal domain of $GABA_{B1}$ (GST-GB1) or $GABA_{B2}$ (GST-GB2) and whole-brain lysates. CaMKII bound to a larger extent to GST-GB1 than to GST-GB2. Control assays were with glutathione beads alone or with beads together with GST protein. (*E*) In vitro phosphorylation of GST-fusion proteins with [γ-^{32}P]-ATP in the presence or absence of recombinant CaMKII. Phosphorylated proteins were separated by SDS/PAGE and exposed to autoradiography. CaMKII specifically phosphorylated GST-GB1 but not GST-GB2 or GST alone. Coomassie blue staining controlled for loading. The GST-GB2 fusion protein tended to degrade (50).

$P < 0.01$). Heteromerization with $GABA_{B2}$ is mandatory for exit of $GABA_{B1}$ from the endoplasmic reticulum and for receptor function (19, 20). As expected from the assembly with $GABA_{B1}$, surface $GABA_{B2}$ protein was also significantly decreased following glutamate or NMDA application, and this decrease was prevented by APV (Fig. S1*A*). We also observed a trend toward decreased surface $GABA_{B1a}$ protein in response to glutamate or NMDA but this did not reach statistical significance (Fig. S1*B*). Although surface biotinylation experiments in cultured cortical neurons revealed significant internalization of endogenous $GABA_{B1b}$ as well as $GABA_{B1a}$ protein in response to NMDA (GB1b NMDA: 52.9 ± 9.9% of control, $n = 3$, $P < 0.01$; GB1a NMDA: 74.1 ± 3.4% of control, $n = 3$, $P < 0.05$; Fig. 2*B*), significantly more $GABA_{B1b}$ than $GABA_{B1a}$ protein was internalized ($P < 0.05$; ANOVA with Bonferroni test). Endogenous surface $GABA_{B2}$ protein was also significantly down-regulated following NMDA treatment (57.0 ± 6.0% of control, $n = 3$, $P < 0.001$; Fig. 2*B*). This supports that preferentially $GABA_{B(1b,2)}$ receptors are removed from the cell surface in response to NMDA application, possibly as a consequence of their selective localization in the somatodendritic compartment (10).

We examined whether the decrease in surface $GABA_{B1b}$ protein following glutamate or NMDA treatment is due to endocytosis. We observed basal endocytosis of surface $GABA_{B1b}$ protein under control conditions (Fig. S2*A*), as previously reported (21). Glutamate or NMDA treatment visibly increased endocytosis of $GABA_{B1b}$ protein, which was inhibited in the presence of APV (Fig. S2*A*). Constitutively internalized $GABA_{B1b}$ protein colocalized with Rab11-eGFP (22, 23), a marker for recycling endosomes (Fig. S2*B*). Following glutamate or NMDA treatment, a fraction of internalized $GABA_{B1b}$ protein segregated into structures devoid of Rab11-eGFP, possibly indicating $GABA_{B1b}$ protein targeted for degradation (24, 25). Preincubation of neurons with dynasore (80 μM for 15 min), a cell-permeable inhibitor of dynamin-dependent endocytosis (26), interfered with the NMDA-mediated removal of surface $GABA_{B1b}$ protein (NMDA: 58.8 ± 5.4% of control, $n = 8$, $P < 0.05$; NMDA + dynasore: 105 ± 10% of control, $n = 10$, $P > 0.05$; dynasore: 98.4 ± 9.0% of control, $n = 9$, $P > 0.05$; Fig. 1*C*). Agonists accelerate basal endocytosis of $GABA_B$ receptors (25). Antagonizing $GABA_B$ receptor activity with CGP54626A (2 μM for 10 min) did not attenuate NMDA-mediated removal of surface $GABA_{B1b}$ protein (NMDA + CGP54626A: 60.2 ± 9.6% of control, $n = 10$, $P < 0.05$; Fig. 1*C*). Thus NMDA receptor activation triggers dynamin-dependent endocytosis of $GABA_B$ receptors, irrespective of whether $GABA_B$ receptors are active or not.

Removal of Surface $GABA_B$ Receptors Requires CaMKII Activity. NMDA failed to reduce surface $GABA_{B1b}$ protein in transfected hippocampal neurons in the presence of the membrane-permeable Ca^{2+}-chelator EGTA-AM (100 μM for 10 min; NMDA: 51.7 ± 6.7% of control, $n = 10$, $P < 0.01$; NMDA + EGTA-AM: 83.4 ± 9.0% of control, $n = 9$, $P > 0.05$; Fig. 2*A*). NMDA also failed to reduce surface $GABA_{B1b}$ protein in the presence of the CaMKII inhibitor KN-93 (10 μM for 10 min; NMDA + KN-93: 85.6 ± 11.1% of control, $n = 10$, $P > 0.05$), implicating activation of CaMKII by NMDA receptors (27) in the removal of surface $GABA_{B1b}$. Likewise, KN-93 also prevented the NMDA-induced decrease of exogenous $GABA_{B2}$ protein (Fig. S1*A*). In contrast, the NMDA-mediated decrease in surface $GABA_{B1b}$ protein was not inhibited in the presence of KN-92 (28), an inactive structural analog of KN-93 (10 μM for 10 min; NMDA + KN-92: 48.9 ± 7.9% of control, $n = 9$, $P < 0.01$; Fig. 2*A*). Biotinylation experiments with cultured cortical neurons demonstrated that surface levels of endogenous $GABA_B$ subunits were significantly less reduced when NMDA was applied in the presence of KN-93 (GB1b: 80.3 ± 6.2% of control, $P > 0.05$ versus control, $P < 0.05$ versus NMDA alone; GB1a: 91.7 ± 4.1% of control, $P > 0.05$ versus control, $P < 0.05$ versus NMDA; GB2: 89.2 ± 3.0% of control, $P > 0.05$ versus control, $P < 0.01$ versus NMDA; $n = 3$; ANOVA with Tukey's multiple comparison test; Fig. 2*B*). Thus KN-93 also interferes with NMDA-mediated internalization of endogenous $GABA_B$ subunits.

S867 in $GABA_{B1}$ Is Phosphorylated by CaMKII. Both anti-$GABA_{B1}$ and anti-$GABA_{B2}$ antibodies efficiently coimmunoprecipitated CaMKII from purified mouse brain membranes, whereas control sera did not (Fig. 2*C*). This indicates that CaMKII associates with the $GABA_{B1}$ and/or $GABA_{B2}$ subunits of heteromeric $GABA_B$ receptors (29). We corroborated this finding by performing pull-down assays with GST fusion proteins encoding the $GABA_{B1}$ and $GABA_{B2}$ C-termini (GST-GB1, GST-GB2). CaMKII in whole-brain lysate associated to a larger extent with GST-GB1 than with GST-GB2, supporting that CaMKII preferentially associates with $GABA_{B1}$ (Fig. 2*D*). For in vitro phosphorylation, the GST-fusion proteins were incubated for 30 min at 30 °C with [γ-^{32}P]-ATP and recombinant CaMKII. CaMKII-dependent phosphorylation was detectable on GST-GB1 but not on GST-GB2 or GST alone (Fig. 2*E*). Thus CaMKII associates with native $GABA_B$ receptors and phosphorylates site(s) in the C terminus of $GABA_{B1}$.

To identify the CaMKII phosphorylation site(s) in $GABA_{B1}$, we digested phosphorylated GST-GB1 protein with LysC and trypsin, separated the resulting peptides by reverse-phase HPLC (RP-HPLC) and collected fractions at 1-min intervals (Fig. 3*A*). The majority of radiolabel eluted in a single peak in fraction 54, which we further analyzed using electrospray ionization mass spectrometry (ESI-MS/MS). Database searches of the ESI-MS/MS scans revealed the presence of the phosphopeptide GEWQSETQDTMK (the methionine of which was oxidized). The fragmentation spectrum indicated phosphorylation of the serine residue corresponding to S867 in the full-length $GABA_{B1a}$ protein (Fig. 3*B*). S867 is localized in the juxtamembrane domain, a regulatory region for many transmembrane proteins, including G-protein–coupled receptors (30). S867 does not conform to the consensus sequence for phosphorylation by CaMKII (31) or other kinases (Table S1). Nonetheless, alanine substitution of putative phosphorylation sites within the GEWQSETQDTMK motif (GST-GB1S867A, GST-GB1T869A, GST-GB1T872A, GST-GB1T869A/T872A) confirmed that recombinant CaMKII only phosphorylates S867 in this sequence (Fig. 3*C*). In addition, we found that CaMKII in brain extracts also specifically phosphorylates S867 in GST-GB1 (Fig. S3).

NMDA Increases Phosphorylation at S867 in Native $GABA_B$ Receptors. To analyze S867 phosphorylation in native tissue, we generated a S867 phosphorylation-state specific antibody, anti-GB1pS867. After phosphorylation of GST fusion proteins with recombinant CaMKII this antibody labeled GST-GB1 but not GST-GB1S867A (Fig. S4*A*). No S867 phosphorylation was seen when using recombinant PKC instead of CaMKII for phosphorylation (Fig. S4*B*). Importantly, the anti-GB1pS867 antibody revealed weak basal S867 phosphorylation (*i*) in mouse brain membranes after enrichment of $GABA_B$ receptors by immunoprecipitation and (*ii*) in synaptic plasma membranes after subcellular fractionation (Fig. 4 *A* and *B*). Application of NMDA to cultured cortical neurons significantly increased phosphorylation of S867 (Fig. 4*C*). Phosphorylation of S867 in brain membranes or cortical neurons was detectable only in the $GABA_{B1b}$ subunit isoform. However, we cannot exclude that NMDA treatment also weakly phosphorylates the $GABA_{B1a}$ subunit and that this phosphorylation is below our detection limit. Of note, $GABA_{B(1b,2)}$ but not $GABA_{B(1a,2)}$ receptors reside in spines (10) where NMDA and $GABA_B$ receptors are particularly abundant

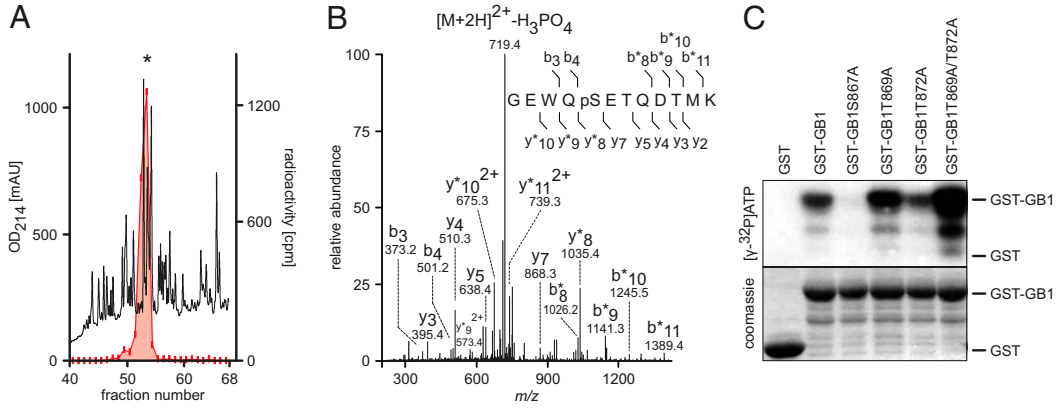

Fig. 3. CaMKII phosphorylates S867 in the $GABA_{B1}$ subunit. (*A*) RP-HPLC analysis of proteolytically digested GST-GB1 after phosphorylation with recombinant CaMKII and [γ-^{32}P]-ATP. Peptide elution was monitored at 214 nm and radioactivity (red) determined by liquid scintillation counting. Asterisk marks elution of the ^{32}P-labeled peptide in fraction 54. (*B*) Fragmentation spectrum of the doubly charged 768.29 Da precursor from the phosphorylated peptide of fraction 54. Fragmentation pattern agrees with predicted ESI-MS/MS spectrum for the phosphopeptide GEWQpS^{867}ETQDTMK. The y- and b-ions matching the GEWQpS^{867}ETQDTMK sequence are labeled. Asterisks mark phosphorylated ions. (*C*) In vitro phosphorylation of GST fusion proteins with recombinant CaMKII and [γ-^{32}P]-ATP. Phosphorylated proteins were separated by SDS/PAGE and exposed to autoradiography. Substitution of S867 with alanine in GST-GB1S867A prevented phosphorylation by CaMKII, whereas alanine substitutions of other putative phosphorylation sites in proximity of S867 (GST-GB1T869A, GST-GB1T872A and GST-GB1T869A/T872A) did not. Coomassie blue staining controlled for loading.

(15). This may explain why NMDA receptor activation preferentially targets $GABA_{B1b}$ for phosphorylation.

Removal of Surface $GABA_B$ Receptors Requires S867 Phosphorylation. Cultured hippocampal neurons expressing HA-GB1b-eGFP or HA-GB1bS867A-eGFP in combination with exogenous $GABA_{B2}$ were analyzed for surface expression of transfected $GABA_{B1b}$ protein (Fig. 4*D* and Fig. S5). HA-GB1bS867A-eGFP exhibited a similar surface expression level as HA-GB1b-eGFP, showing that lack of S867 phosphorylation does not prevent surface expression. However, HA-GB1bS867A-eGFP was refractory to removal from the surface upon NMDA treatment, as determined by the ratio of surface to total fluorescence intensity (GB1b NMDA: $52.6 \pm 4.8\%$, $n = 10, P < 0.01$; GB1bS867A control: $82.4 \pm 6.3\%, n = 9, P > 0.05$; GB1bS867A NMDA: $98.1 \pm 16.0, n = 8, P > 0.05$; data normalized to GB1b control; Fig. 4*D*). This implicates S867 phosphorylation in $GABA_B$ receptor removal from the cell surface.

NMDA-Mediated CaMKII Activation Reduces $GABA_B$-Induced K^+ Currents. Well-known effectors of dendritic $GABA_B$ receptors are the Kir3-type K^+ channels, which cluster with $GABA_B$ receptors in spines (12). We used whole-cell patch-clamp recording to address whether NMDA-treatment reduces baclofen-induced K^+ currents due to $GABA_B$ receptor internalization. Baclofen-evoked K^+ currents were recorded from cultured hippocampal neurons clamped at −50 mV after pharmacological blockade of Na^+ channels, $GABA_A$, glycine, α-amino-3-hydroxy-5-methyl-isoxazole-4-propionic acid (AMPA) and kainate receptors (Fig. 5*A*). Baclofen-induced K^+ currents were recorded before and 30 min after NMDA treatment (30 μM NMDA/5 μM glycine in Mg^{2+}-free solution for 1 min). During NMDA applications, neurons were held at −70 mV to minimize Ca^{2+} entry through voltage-gated Ca^{2+} channels. Following NMDA treatment, the maximal amplitudes of the baclofen-induced K^+ currents were reduced ($19.1 \pm 6.5\%$, $n = 5$; Fig. 5*C*). Likewise, baclofen-induced K^+ currents was decreased following glutamate treatment (5 μM glutamate/5 μM glycine in Mg^{2+}-free solution for 1 min; $35.2 \pm 5.1\%$, $n = 3$), and this decrease was prevented by the NMDA-receptor antagonist dCPP (20 μM; $93.5 \pm 0.5\%, n = 3, P < 0.001$ compared with NMDA alone; Fig. 5 *A* and *C*). Intracellular dialysis with the CaMKII inhibitor KN-93 (5 μM) significantly attenuated the NMDA-mediated reduction of K^+ currents ($65.5 \pm 9.0\%$, $n = 5$, $P < 0.001$ compared with NMDA alone). Ca^{2+}/calmodulin-dependent protein kinase kinase β (CaMKKβ) promotes phosphorylation of the $GABA_{B2}$ subunit by 5′AMP-dependent protein kinase (32). Intracellular dialysis with the CaMKK inhibitor STO-609 (5 μM) resulted in a modest attenuation of NMDA-mediated reduction of K^+-currents that, however, did not reach significance ($41.3 \pm 2.9\%, n = 5, P > 0.05$ compared with NMDA alone; Fig. 5 *A* and *C*). We next addressed whether phosphorylation at S867 is critical for the NMDA-mediated decrease in K^+-current amplitude. We transfected cultured hippocampal neurons from $GABA_{B1}{}^{-/-}$ ($GB1^{-/-}$) mice (33) with expression constructs for $GABA_{B1b}$ (GB1b), $GABA_{B1a}$ (GB1a) or GB1bS867A. All exogenous $GABA_{B1}$ subunits, including GB1bS867A, fully rescued $GABA_B$ receptor function, demonstrating that they heteromerize with endogenous $GABA_{B2}$ subunits (Fig. 5 *B* and *D*). In $GB1^{-/-}$ neurons reconstituted with GB1b, NMDA application decreased the baclofen-induced K^+ currents to a similar extent as in wild-type neurons. In contrast, in $GB1^{-/-}$ neurons reconstituted with GB1a or GB1bS867A NMDA application decreased the K^+ currents significantly less (GB1b: $28.3 \pm 3.0\%$, $n = 5$; GB1a: $54.2 \pm 7.2\%, n = 6, P < 0.05$; GB1bS867A: $64.1 \pm 7.0\%$,

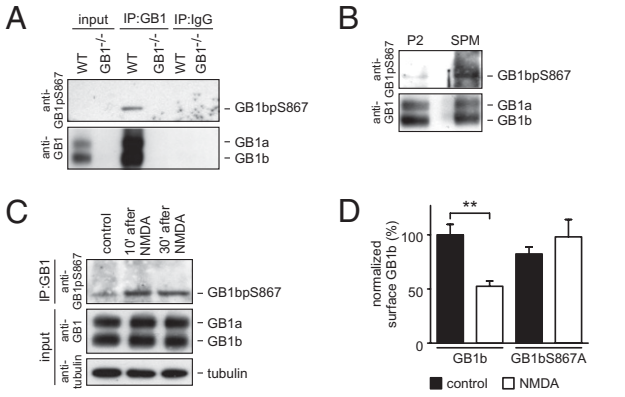

Fig. 4. S867 phosphorylation in brain tissue and cultured neurons. (*A*) S867 phosphorylation was detectable after immunoprecipitation of $GABA_B$ receptors with anti-$GABA_{B1}$ antibodies (IP:GB1) from WT but not $GB1^{-/-}$ brain membranes. S867 phosphorylation was detected on Western blots with a phosphorylation-state specific antibody (anti-GB1pS867). The same blot was reprobed with anti-GB1 antibodies. Immunoprecipitation with rabbit IgG (IP:IgG) was used as a control. Note the specific phosphorylation of the $GABA_{B1b}$ subunit. (*B*) S867 phosphorylation of $GABA_{B1b}$ was clearly detectable in synaptic plasma membranes (SPM) and barely detectable in the P2 membrane fraction purified from total mouse brain homogenates. (*C*) NMDA application to cultured cortical neurons increased S867 phosphorylation in the $GABA_{B1b}$ subunit. Neurons were treated with NMDA for 3 min and harvested at the times indicated. Whole-cell lysates (input) were subjected to immunoprecipitation with anti-GB1 antibodies (IP:GB1). S867 phosphorylation was detected on Western blot with anti-GB1pS867; anti-tubulin antibodies were used as control. (*D*) Alanine mutation of S867 in $GABA_{B1b}$ prevents NMDA-induced internalization. Cultured hippocampal neurons expressing exogenous HA-GB1b-eGFP (GB1b) or HA-GB1bS867A-eGFP (GB1bS867A) together with $GABA_{B2}$ were analyzed at DIV14. Surface $GABA_{B1b}$ protein was quantified by the ratio of surface to total fluorescence intensity. Values were normalized to GB1b control in the absence of NMDA. Data are means ± SEM, n = 8–10. $^{**}P < 0.01$.

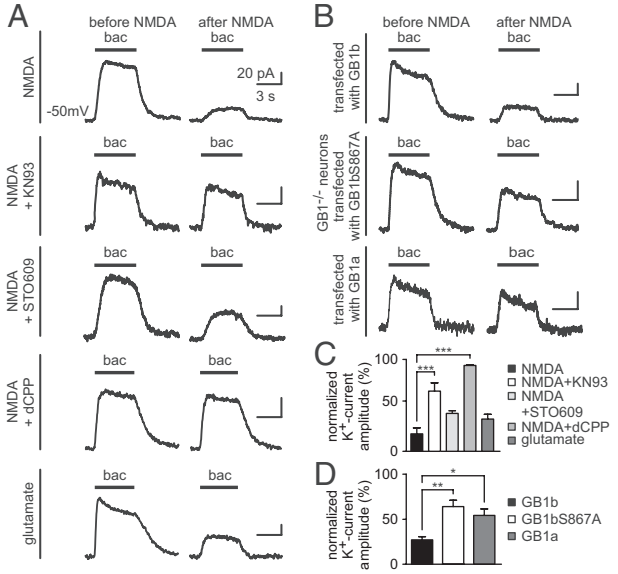

Fig. 5. CaMKII reduces $GABA_B$-mediated K^+ currents in cultured hippocampal neurons. (*A*) Representative baclofen-induced K^+ currents recorded at −50 mV before and after application of NMDA or glutamate. Baclofen-induced K^+ currents were strongly reduced 30 min after NMDA or glutamate application. KN-93 and dCPP but not STO-609 attenuated the NMDA-mediated K^+ current reduction. (*B*) Representative baclofen-induced K^+ currents recorded from neurons of $GABA_{B1}{}^{-/-}$ ($GB1^{-/-}$) mice transfected with $GABA_{B1a}$ (GB1a) $GABA_{B1b}$, (GB1b) or GB1bS867A expression vectors. NMDA was less effective in decreasing the K^+ current in neurons transfected with GB1bS867A or $GABA_{B1a}$. (*C*) Bar graph illustrating that dCPP and KN-93 attenuated the NMDA-mediated reduction of baclofen-induced K^+ currents. (*D*) NMDA was significantly less effective in decreasing the K^+ current in $GB1^{-/-}$ neurons transfected with GB1a or GB1bS867A than with GB1b. Maximal K^+-current amplitudes after NMDA application were normalized to the maximal K^+-current amplitudes before NMDA application. Data are means ± SEM, n = 3–6. $^{*}P < 0.05$; $^{**}P < 0.01$; $^{***}P < 0.001$.

$n = 5, P < 0.01$). Thus predominantly phosphorylation of $GABA_{B1b}$ at S867 is implicated in the NMDA-mediated decrease of the K^+-current amplitude.

NMDA-Mediated Endocytosis of $GABA_B$ Receptors in Dendritic Shafts and Spines. $GABA_{B(1b,2)}$ receptors, which appear to be the main substrate for S867 phosphorylation, resides in dendritic spines and shafts (10). We therefore addressed whether $GABA_B$ receptors at these locations internalize in response to NMDA. We transfected $GABA_{B1b}$ fused to a pH-sensitive eGFP [Super Ecliptic pHluorin (SEP-GB1b)] together with $GABA_{B2}$ into organotypic hippocampal slice cultures. SEP-GB1b selectively visualizes $GABA_{B1b}$ protein at the cell surface (34). In addition, we expressed the freely diffusible red fluorescent protein (RFP) t-dimer2 to visualize the morphology of transfected cells (10). Time-lapse two-photon images of transfected CA1 pyramidal cells were collected at days in vitro (DIV) 14–21 (Fig. 6*A*). Dendrites were imaged at 5-min intervals before and after bath application of NMDA (30 μM for 1 min). NMDA application resulted in a long-lasting decrease in green fluorescence in dendritic spines and shafts, indicating $GABA_B$ receptor internalization (Fig. 6 *B* and *C*, green traces; SEP-GB1b fluorescence ratio after/before NMDA: spine, $0.82 \pm 0.05, n = 22, P < 0.001$; shaft, $0.73 \pm 0.04, n = 8, P < 0.001$; nonparametric Mann–Whitney test; five cells analyzed). NMDA application did not significantly affect RFP fluorescence in dendritic spines and shafts (Fig. 6 *B* and *C*, red traces; RFP fluorescence ratio after/before NMDA: spine, $1.04 \pm 0.05, n = 22, P > 0.05$; shaft, $0.88 \pm 0.03, n = 8, P > 0.05$). The decrease in green fluorescence was inhibited in the presence of the NMDA receptor antagonist dCPP (20 μM; Fig. 6 *B* and C, green traces; SEP-GB1b fluorescence ratio after/before NMDA: spine, $1.00 \pm 0.05, n = 15, P > 0.05$; shaft, $0.99 \pm 0.04, n = 3, P > 0.05$; 2 cells analyzed). No significant change in the red fluorescence under NMDA receptor blockade was observed (Fig. 6 *B* and C, red traces; RFP fluorescence ratio after/before NMDA: spine, $1.06 \pm 0.07, n = 15, P > 0.05$; shaft, $1.02 \pm 0.03, n = 3, P > 0.05$). Thus NMDA receptor stimulation leads to $GABA_B$ receptor internalization in dendritic spines and shafts. In agreement with experiments described above (Figs. 4*D* and 5*D* and Fig. S5*B*) the SEP-GB1bS867A protein is refractory to NMDA-induced internalization in dendritic spines and shafts (Fig. S6).

Discussion

Activity-Dependent Phosphorylation and Internalization of Dendritic $GABA_B$ Receptors. A previous report showed that glutamate application to cortical neurons decreases the number of $GABA_B$ receptors at the cell surface (18). Another report showed that glutamate application increases the steady-state level of $GABA_B$ receptor endocytosis while at the same time reducing the rate of endocytosis (35). Here, we show that glutamate acts via NMDA receptors to activate CaMKII (36), which directly phosphorylates S867 in the C terminus of $GABA_{B1}$ to trigger endocytosis. NMDA-dependent phosphorylation of S867 is detectable only in the $GABA_{B1b}$ subunit, which mostly resides in the dendrites and, in contrast to the $GABA_{B1a}$ subunit, efficiently penetrates spines (10). Consistent with this, we found that $GABA_B$ receptors undergo endocytosis in dendritic spines and shafts within minutes of NMDA receptor activation. Notably, endocytosis prevents $GABA_B$ receptors from activating effector K^+ channels that cluster with $GABA_B$ receptors in spines (12).

Physiological Implications. GABA from interneurons firing in synchrony can spill over to pre- and postsynaptic $GABA_B$ receptors on excitatory synapses (11, 37). This will reduce glutamate release and produce hyperpolarizing inhibitory postsynaptic potentials that enhance Mg^{2+} block of NMDA receptors and thus reduce their Ca^{2+} signals (13, 14). In addition to modulating the electrical properties of neurons, $GABA_B$ receptors can also reduce the Ca^{2+} permeability of NMDA receptors in dendritic spines via activation of the PKA signaling pathway (15). Here, we demonstrate that NMDA receptors can counter this suppression of Ca^{2+} signals and rapidly endocytose $GABA_B$ receptors from the surface of dendritic shafts and spines. Hence, there appears to be a reciprocal regulation where both NMDA and $GABA_B$ receptors can cancel each other out. The temporal interplay of NMDA and $GABA_B$ receptors may be particularly relevant to phenomena controlling synaptic strength, where NMDA receptor activity is of importance. Of note, the same NMDA receptor/CaMKII signaling cascade regulating synaptic strength also internalizes $GABA_B$ receptors. This provides a means to keep individual glutamatergic synapses modifiable (38, 39) and to spare them from inhibition through spillover of GABA. A previous study reported that NMDA receptor activation promotes surface expression of Kir3 channels in hippocampal neurons (40), which was paralleled with an increase in basal Kir3 currents and adenosine A_1-mediated Kir3 currents (41). However, $GABA_B$ mediated Kir3 currents were not altered, in apparent conflict with an earlier report (42) and our own findings. The reasons for these discrepancies are unclear but may relate to differences in the signaling pathways activated under the different experimental conditions used. Reciprocal regulation of NMDA and $GABA_B$ receptors is reminiscent of the recently

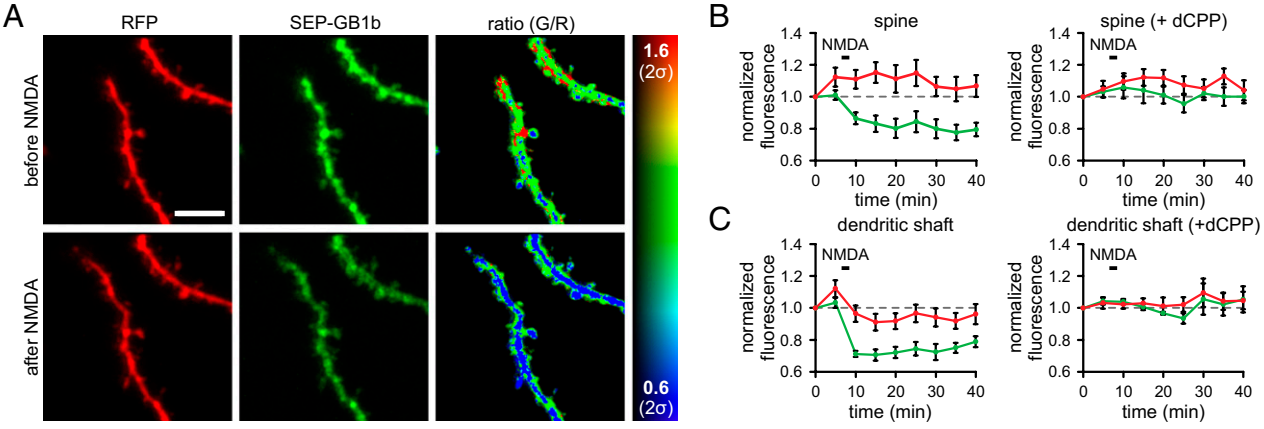

Fig. 6. NMDA-mediated endocytosis of $GABA_B$ receptors in dendritic spines and shafts. (*A*) Red fluorescence (R), green fluorescence (G), and G/R ratio images of dendrites expressing freely diffusible RFP and SEP-GB1b before and after NMDA application. NMDA application leads to a decrease in green fluorescence in dendritic spines and shafts. G/R ratio is coded in rainbow colors and is scaled to encompass 2 SDs (2σ) of the average dendritic ratio before NMDA application. (Scale bar, 5 μm.) (*B* and *C*) Time course of red and green fluorescence in dendritic spines (*B*) and shafts (*C*) before and after NMDA application. NMDA leads to a long-lasting decrease in SEP-fluorescence within minutes, which is prevented by prior application of dCPP. Data are mean ± SEM.

reported interplay of NMDA and muscarinic receptors (43). In this cross-talk, NMDA receptors phosphorylate and inactivate muscarinic receptors in a CaMKII-dependent manner, much in the same way as now observed with $GABA_B$ receptors.

Materials and Methods

Neuronal Cultures. Dissociated hippocampal and cortical neurons were prepared from embryonic day 18.5 Wistar rats or from embryonic day 16.5 WT and $GABA_{B1}^{-/-}$ mice (33, 44). Neurons were transfected at DIV7 using Lipofectamin 2000 (Invitrogen). Pharmacological treatments were performed in conditioned medium at 37 °C/5% CO_2.

Biochemistry. Surface biotinylation, immunoprecipitation, in vitro phosphorylation, HPLC analysis, and MS were essentially performed as described (24, 45, 46).

Electrophysiology. Recordings in cultured hippocampal neurons were performed with an Axopatch 200B patch-clamp amplifier. $GABA_B$ responses were evoked by fast application of 100 μM baclofen (47).

Two-Photon Imaging. Organotypic hippocampal slice cultures for two-photon time-lapse imaging (48) were prepared from Wistar rats at postnatal day 5 (49). For time-lapse imaging, we used a custom-built, two-photon laser scanning microscope based on a BX51WI microscope (Olympus) and a pulsed Ti:Sapphire laser (Chameleon XR, Coherent) tuned to λ = 930 nm, controlled by the open source software ScanImage. Fluorescence was detected in epi- and trans-fluorescence mode using four photomultiplier tubes (R2896, Hamamatsu).

Data Analysis. Data are given as mean ± SEM. Statistical significance was assessed using ANOVA, with the Dunnett's multiple comparison test unless otherwise indicated, using GraphPad Prism 5.0.

Additional experimental procedures are described in *SI Materials and Methods*.

ACKNOWLEDGMENTS. We thank N. Hardel (Department of Biomedicine, Institute of Physiology, Pharmazentrum, University of Basel, Basel, Switzerland) for the Rab11-eGFP plasmid, K. Ivankova and A. Cremonesi for technical help, and F. Schatzmann for comments on the manuscript. B.B. was supported by the Swiss Science Foundation (3100A0-117816) and the European Community's Seventh Framework Programme FP7/2007-2013 under Grant Agreement 201714. R.T. was supported by the Wellcome Trust International Senior Research Fellowship and an EU Synapse grant (LSHM-CT-2005-019055).

1. Bettler B, Kaupmann K, Mosbacher J, Gassmann M (2004) Molecular structure and physiological functions of $GABA_B$ receptors. *Physiol Rev* 84:835–867.
2. Couve A, Moss SJ, Pangalos MN (2000) $GABA_B$ receptors: A new paradigm in G protein signaling. *Mol Cell Neurosci* 16:296–312.
3. Ulrich D, Bettler B (2007) $GABA_B$ receptors: Synaptic functions and mechanisms of diversity. *Curr Opin Neurobiol* 17:298–303.
4. Kornau HC (2006) $GABA_B$ receptors and synaptic modulation. *Cell Tissue Res* 326: 517–533.
5. Jarolimek W, Misgeld U (1997) $GABA_B$ receptor-mediated inhibition of tetrodotoxin-resistant GABA release in rodent hippocampal CA1 pyramidal cells. *J Neurosci* 17: 1025–1032.
6. Scanziani M, Capogna M, Gähwiler BH, Thompson SM (1992) Presynaptic inhibition of miniature excitatory synaptic currents by baclofen and adenosine in the hippocampus. *Neuron* 9:919–927.
7. Lüscher C, Jan LY, Stoffel M, Malenka RC, Nicoll RA (1997) G protein-coupled inwardly rectifying K^+ channels (GIRKs) mediate postsynaptic but not presynaptic transmitter actions in hippocampal neurons. *Neuron* 19:687–695.
8. Marshall FH, Jones KA, Kaupmann K, Bettler B (1999) $GABA_B$ receptors—the first 7TM heterodimers. *Trends Pharmacol Sci* 20:396–399.
9. Biermann B, et al. (2010) The Sushi domains of $GABA_B$ receptors function as axonal targeting signals. *J Neurosci* 30:1385–1394.
10. Vigot R, et al. (2006) Differential compartmentalization and distinct functions of $GABA_B$ receptor variants. *Neuron* 50:589–601.
11. Guetg N, et al. (2009) The $GABA_{B1a}$ isoform mediates heterosynaptic depression at hippocampal mossy fiber synapses. *J Neurosci* 29:1414–1423.
12. Kulik A, et al. (2006) Compartment-dependent colocalization of Kir3.2-containing K^+ channels and $GABA_B$ receptors in hippocampal pyramidal cells. *J Neurosci* 26:4289–4297.
13. Morrisett RA, Mott DD, Lewis DV, Swartzwelder HS, Wilson WA (1991) $GABA_B$-receptor-mediated inhibition of the N-methyl-D-aspartate component of synaptic transmission in the rat hippocampus. *J Neurosci* 11:203–209.
14. Otmakhova NA, Lisman JE (2004) Contribution of I_h and $GABA_B$ to synaptically induced afterhyperpolarizations in CA1: A brake on the NMDA response. *J Neurophysiol* 92: 2027–2039.
15. Chalifoux JR, Carter AG (2010) $GABA_B$ receptors modulate NMDA receptor calcium signals in dendritic spines. *Neuron* 66:101–113.
16. Cimarosti H, Kantamneni S, Henley JM (2009) Ischaemia differentially regulates $GABA_B$ receptor subunits in organotypic hippocampal slice cultures. *Neuropharmacol* 56:1088–1096.
17. Straessle A, Loup F, Arabadzisz D, Ohning GV, Fritschy JM (2003) Rapid and long-term alterations of hippocampal $GABA_B$ receptors in a mouse model of temporal lobe epilepsy. *Eur J Neurosci* 18:2213–2226.
18. Vargas KJ, et al. (2008) The availability of surface $GABA_B$ receptors is independent of γ-aminobutyric acid but controlled by glutamate in central neurons. *J Biol Chem* 283: 24641–24648.
19. Pagano A, et al. (2001) C-terminal interaction is essential for surface trafficking but not for heteromeric assembly of $GABA_B$ receptors. *J Neurosci* 21:1189–1202.
20. Margeta-Mitrovic M, Jan YN, Jan LY (2000) A trafficking checkpoint controls $GABA_B$ receptor heterodimerization. *Neuron* 27:97–106.
21. Grampp T, Sauter K, Markovic B, Benke D (2007) γ-Aminobutyric acid type B receptors are constitutively internalized via the clathrin-dependent pathway and targeted to lysosomes for degradation. *J Biol Chem* 282:24157–24165.
22. Hardel N, Harmel N, Zolles G, Fakler B, Klöcker N (2008) Recycling endosomes supply cardiac pacemaker channels for regulated surface expression. *Cardiovasc Res* 79:52–60.
23. Maxfield FR, McGraw TE (2004) Endocytic recycling. *Nat Rev Mol Cell Biol* 5:121–132.
24. Fairfax BP, et al. (2004) Phosphorylation and chronic agonist treatment atypically modulate $GABA_B$ receptor cell surface stability. *J Biol Chem* 279:12565–12573.
25. Grampp T, Notz V, Broll I, Fischer N, Benke D (2008) Constitutive, agonist-accelerated, recycling and lysosomal degradation of $GABA_B$ receptors in cortical neurons. *Mol Cell Neurosci* 39:628–637.
26. Macia E, et al. (2006) Dynasore, a cell-permeable inhibitor of dynamin. *Dev Cell* 10:839–850.
27. Lisman J, Schulman H, Cline H (2002) The molecular basis of CaMKII function in synaptic and behavioural memory. *Nat Rev Neurosci* 3:175–190.
28. Tombes RM, Grant S, Westin EH, Krystal G (1995) G_1 cell cycle arrest and apoptosis are induced in NIH 3T3 cells by KN-93, an inhibitor of CaMK-II (the multifunctional Ca^{2+}/CaM kinase). *Cell Growth Differ* 6:1063–1070.
29. Kaupmann K, et al. (1998) $GABA_B$-receptor subtypes assemble into functional heteromeric complexes. *Nature* 396:683–687.
30. Kim CH, Lee J, Lee JY, Roche KW (2008) Metabotropic glutamate receptors: Phosphorylation and receptor signaling. *J Neurosci Res* 86:1–10.
31. Pearson RB, Woodgett JR, Cohen P, Kemp BE (1985) Substrate specificity of a multifunctional calmodulin-dependent protein kinase. *J Biol Chem* 260:14471–14476.
32. Kuramoto N, et al. (2007) Phospho-dependent functional modulation of $GABA_B$ receptors by the metabolic sensor AMP-dependent protein kinase. *Neuron* 53:233–247.
33. Schuler V, et al. (2001) Epilepsy, hyperalgesia, impaired memory, and loss of pre- and postsynaptic $GABA_B$ responses in mice lacking $GABA_{B(1)}$. *Neuron* 31:47–58.
34. Kopec CD, Li B, Wei W, Boehm J, Malinow R (2006) Glutamate receptor exocytosis and spine enlargement during chemically induced long-term potentiation. *J Neurosci* 26:2000–2009.
35. Wilkins ME, Li X, Smart TG (2008) Tracking cell surface $GABA_B$ receptors using an alpha-bungarotoxin tag. *J Biol Chem* 283:34745–34752.
36. Nicoll RA, Malenka RC (1999) Expression mechanisms underlying NMDA receptor-dependent long-term potentiation. *Ann N Y Acad Sci* 868:515–525.
37. Scanziani M (2000) GABA spillover activates postsynaptic $GABA_B$ receptors to control rhythmic hippocampal activity. *Neuron* 25:673–681.
38. Lee SJ, Escobedo-Lozoya Y, Szatmari EM, Yasuda R (2009) Activation of CaMKII in single dendritic spines during long-term potentiation. *Nature* 458:299–304.
39. Zhang YP, Holbro N, Oertner TG (2008) Optical induction of plasticity at single synapses reveals input-specific accumulation of alphaCaMKII. *Proc Natl Acad Sci USA* 105:12039–12044.
40. Chung HJ, Qian X, Ehlers M, Jan YN, Jan LY (2009) Neuronal activity regulates phosphorylation-dependent surface delivery of G protein-activated inwardly rectifying potassium channels. *Proc Natl Acad Sci USA* 106:629–634.
41. Chung HJ, et al. (2009) G protein-activated inwardly rectifying potassium channels mediate depotentiation of long-term potentiation. *Proc Natl Acad Sci USA* 106:635–640.
42. Huang CS, et al. (2005) Common molecular pathways mediate long-term potentiation of synaptic excitation and slow synaptic inhibition. *Cell* 123:105–118.
43. Butcher AJ, et al. (2009) N-methyl-D-aspartate receptors mediate the phosphorylation and desensitization of muscarinic receptors in cerebellar granule neurons. *J Biol Chem* 284:17147–17156.
44. Brewer GJ, Torricelli JR, Evege EK, Price PJ (1993) Optimized survival of hippocampal neurons in B27-supplemented Neurobasal, a new serum-free medium combination. *J Neurosci Res* 35:567–576.
45. Gassmann M, et al. (2004) Redistribution of $GABA_{B(1)}$ protein and atypical $GABA_B$ responses in $GABA_{B(2)}$-deficient mice. *J Neurosci* 24:6086–6097.
46. Gander S, et al. (2008) Identification of the rapamycin-sensitive phosphorylation sites within the Ser/Thr-rich domain of the yeast Npr1 protein kinase. *Rapid Commun Mass Spectrom* 22:3743–3753.
47. Schwenk J, et al. (2010) Native $GABA_B$ receptors are heteromultimers with a family of auxiliary subunits. *Nature* 465:231–235.
48. Holbro N, Grunditz A, Oertner TG (2009) Differential distribution of endoplasmic reticulum controls metabotropic signaling and plasticity at hippocampal synapses. *Proc Natl Acad Sci USA* 106:15055–15060.
49. Stoppini L, Buchs PA, Muller D (1991) A simple method for organotypic cultures of nervous tissue. *J Neurosci Methods* 37:173–182.
50. Couve A, et al. (2002) Cyclic AMP-dependent protein kinase phosphorylation facilitates $GABA_B$ receptor-effector coupling. *Nat Neurosci* 5:415–424.